AIP | Review of Scientific Instruments

Fabrication of petal-shaped masks for suppression of the on-axis Poisson spot in telescope systems

Ron Shiri, Ryan Stein, Kaitlin Murphy, Kimberly Hagopian, Shirin Salari, Shannon Sankar, John Hagopian, Matthew Showalter, Thomas Stevenson, Manuel Quijada, Felix Threat, Jay Friedlander, Thomas Dillon, and Jeffrey Livas

Citation: Review of Scientific Instruments **87**, 043112 (2016); doi: 10.1063/1.4945793
View online: http://dx.doi.org/10.1063/1.4945793
View Table of Contents: http://scitation.aip.org/content/aip/journal/rsi/87/4?ver=pdfcov
Published by the AIP Publishing

Fabrication of petal-shaped masks for suppression of the on-axis Poisson spot in telescope systems

Ron Shiri,[1] Ryan Stein,[2] Kaitlin Murphy,[1] Kimberly Hagopian,[1] Shirin Salari,[1] Shannon Sankar,[2,3] John Hagopian,[1] Matthew Showalter,[4] Thomas Stevenson,[5] Manuel Quijada,[1] Felix Threat,[1] Jay Friedlander,[6] Thomas Dillon,[7] and Jeffrey Livas[2]
[1]*Optics Branch, NASA Goddard Space Flight Center, Greenbelt, Maryland 20771, USA*
[2]*Gravitational Astrophysics Laboratory, NASA Goddard Space Flight Center, Greenbelt, Maryland 20771, USA*
[3]*University Space Research Association, Goddard Space Flight Center, Greenbelt, Maryland 20771, USA*
[4]*Advanced Manufacturing Branch, NASA Goddard Space Flight Center, Greenbelt, Maryland 20771, USA*
[5]*Detector Systems Branch, NASA Goddard Space Flight Center, Greenbelt, Maryland 20771, USA*
[6]*Astrophysics Science Laboratory, NASA Goddard Space Flight Center, Greenbelt, Maryland 20771, USA*
[7]*Department of Electrical and Computer Engineering, University of Delaware, Newark, Delaware 19716, USA*

(Received 8 September 2015; accepted 28 March 2016; published online 19 April 2016)

The presence of a bright (Poisson) spot in the geometrical shadow of circular/spherical shapes has been known for the past two centuries. A broad class of telescopes that involve simultaneous transmit and receive require suppression of the reflected light from the secondary mirror on the detector. For instance, the on-axis design of optical telescope for the evolved Laser Interferometric Space Antenna (eLISA), a re-scoped version of the baseline LISA mission concept, requires suppression of reflected laser light from the secondary mirror on the detector. In the past few years, the hypergaussian functions with petal-shaped realization have been shown to significantly suppress intensity along the optical axis. This work reports on fabrication of a series of petal-shaped masks using a variety of techniques such as 3D printing, photolithography, and wire Electro Discharge Machining. These masks are designed and fabricated to operate in the range of Fresnel numbers between 4 and 120. This paper discusses the challenges, successes, and failures of each fabrication technique and the optical performance of typical masks with suggestions for potential follow up work. [http://dx.doi.org/10.1063/1.4945793]

I. INTRODUCTION

The presence of the Poisson spot (spot of Arago) in a geometrical shadow region can be characterized as the interference of light waves diffracted on the edges of the obscuration with its central position determined by the symmetry of the object. A number of studies in the past few years have looked into the characterization of this spot.[1] More recently, a number of disciplines from photonics to astronomy require suppression of this bright spot. For instance, the exoplanetary missions in search of Earth-like planets using direct imaging techniques require suppression of the broadband bright starlight on the telescope aperture.[2] Additionally, the evolved Laser Interferometric Space Antenna (eLISA), a re-scoped version of the baseline LISA mission concept, if operated with an on-axis telescope design, requires suppression of the directly reflected laser source from the secondary mirror of the telescope assembly back onto the detector.[3] These observatories will study the source of gravitational waves from 0.0001 Hz to 1 Hz by monitoring the path length difference between pairs of free falling test masses with laser interferometry to a precision of picometers over gigameter baselines.[4]

The physical size of the masks required to suppress the Poisson spot can vary over a wide range from mm to 10's of meters depending on the application and where the mask is placed in the optical system. In this work, we have concentrated on developing fabrication techniques for masks with diameters of a few mm intended to be placed on the secondary mirror of a telescope with <0.5 m primary apertures.

The suppression of the Poisson spot using a variety of techniques has received considerable attention in recent years. In particular, and relevant to our work, the hypergaussian function interpretation as petal shapes has been shown to reduce this spot significantly.[5] We have designed a series of symmetrical petal-shaped masks specific to the geometry of the problem by employing the electromagnetic analysis of the shadow behind an object described by the Fresnel number.[6] In this work, we focus on the fabrication of these masks for the suppression of diffraction from a narrow-band incident laser source in order to identify implementation issues that may limit performance other than the specific design of the mask. The goal is to evaluate the fidelity of a fabrication process in order to be able to say quantitatively how well the mask that is actually realized matches the intended design. The optical testbed setup in transmission is fairly straightforward and different fabricated masks could easily be inserted in the optical path to evaluate their performance.

II. FABRICATION TECHNIQUES

To evaluate the fabrication techniques, we designed a series of binary petal shaped masks ranging from 6 to 16 petals with variety of petal tip radius-of-curvature (ROC). Earlier studies showed a direct correlation between the level of suppression on the shadow and sharpness of petal tips.[7] In this work, we designed a series of petal-shape mask for Fresnel numbers 4–120.

In Subsections II A–II E, we describe a variety of techniques employed to fabricate these masks. The techniques range from high-resolution inkjet printing to additive 3D printing, photolithography on fused silica substrates, and wire Electro Discharge Machining (EDM). We did not consider typical mechanical shop fabrication techniques because we expected to need tolerances better than ~2.5 μm (0.0001 in.) tolerances typically achieved. For the purpose of fabrication, the petal-shape mask boundary outline is converted into machine specific file formats. For instance, the digital outline of the mask is converted to the StereoLithography (STL) format for 3D printing, Standard for the Exchange of Product Data (STEP) format for the wire EDM, and Graphic Database System (GDSII) format for the photolithography fabrication. After fabrication, the quality of the masks is inspected under microscope for edge smoothness, geometrical size, and petal tip outer ROC accuracy—all parameters that affect the degree of on-axis suppression.

A. High-resolution printers

An 8-petal mask 50-mm in diameter is designed for high-resolution inkjet printing. The high-resolution (2400 × 1200 dpi) photo printer, HP DesignJet, Z3200, was used for this purpose. This printer has 4.0 pl ink drops and 2112-nozzle print heads. A series of masks with various petal tips were printed. Inspection of the printed masks with a microscope shows rough edges, large spatial gaps between the ink drops and on the surface of the mask and inaccurate petal tips.

B. 3D printers

The same mask design in inkjet printing was used in a 3D printing exercise. However, the diameter of the masks varied from 15 mm to 50 mm to shorten the long fabrication time of 3D printing. The 3D printers used in this exercise are a MakerBot Replicator 2 and an OJECT Eden 260 V. For this purpose, the digital format of the 2D petal mask was converted into an STL file format with z-axis extrusion (thickness) from 0.5 mm to 2 mm. Figure 1 shows the fabricated masks using the OBJET printer. This technology is similar to an inkjet printer but instead of jetting ink onto paper, the printer jets layers of curable photopolymer onto a build tray. The 3D model of a mask is built by accumulation of fine layers of resin into the desired shape once the software reads the STL file.

The petal tip radius is designed in the millimeter range to assess the performance of the printer. The thickness of the fabricated mask ranges from 0.5 mm to 2 mm. A close inspection of the printed mask shows geometrical inaccuracy with respect to the prescribed mask accompanied by rough boundaries that makes the mask impractical for optical testing.

C. Photolithography

Three sets of masks, 2, 5, and 10-mm in diameter were designed with a variety of petal tips. The digital layout of petal masks is arranged along a radial pattern on a circular disk (Figure 2). Each set of petaled masks has an additional reference circular mask to assess the performance of the suppression in the lab experiment. A 4-in. diameter photomask of the patterns with 18 shapes is prepared using E-beam lithography. In the photolithography process, the patterns are transferred from photomask to photoresist on the substrate with sputter deposition of chromium or aluminum. Figure 3 shows a fabricated set of masks on fused silica substrate. In this work, two variables may be adjusted, the thickness and the type of metal used in the deposition. In order to have no signs of transmission through the mask once illuminated with 1064-nm laser source, we employed 300-nm thick aluminum layer coated with 50 Å of MgF3 as anti-reflection (AR) coating on 500-μm thick substrate.

Table I shows the arrangement of the numbered masks on the substrate. Each row contains designed and measured ROC of the petal tips in microns followed by the diameter in millimeters, targeted Fresnel number, and number of petals on the mask. The reference mask number in the first column of this table correlates with the mask numbers on Figure 2.

The hypergaussian function employed for these masks is designed specifically for suppression range of 2–4 orders of

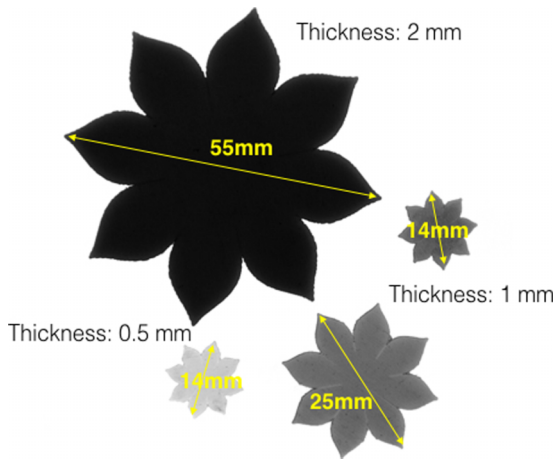

FIG. 1. The OBJET printed masks. The mask diameter range from 15 to 50 mm. The larger mask with 2-mm thick petal mask is darker than the 0.5-mm thick mask.

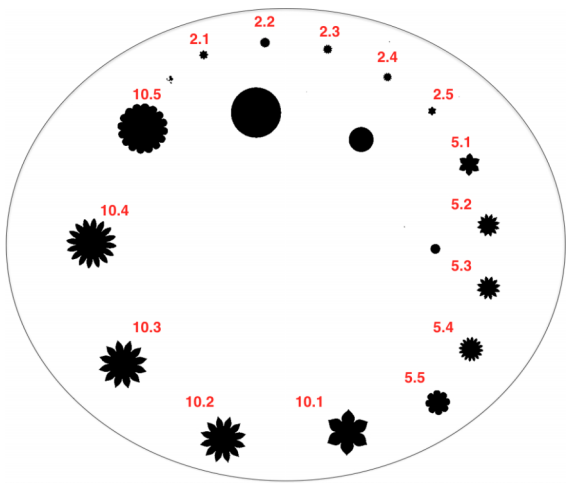

FIG. 2. Petal-shape masks in radial arrangement as fabricated on silica wafer. The red numbers specify mask as described in Table I.

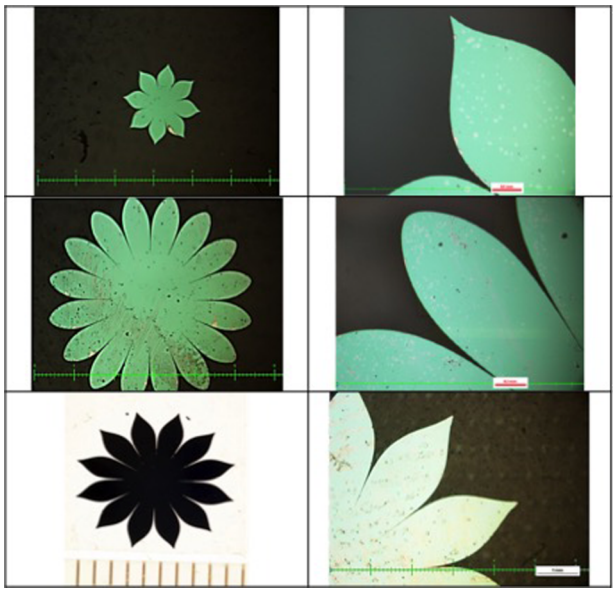

FIG. 3. Microscopic image of fabricated chromium masks on 4×4 in. fused silica substrate. The top row is a 2-mm diameter mask, 6 petals, and 2-μm tips (pmask 2.5). The middle row is a 5-mm diameter mask, 16 petals, and 200-μm tips (pmask 5.4). The bottom row is a 10-mm diameter mask, 12 petals, and 20-μm tips (pmask 10.3). The right column is zoomed microscopic image showing the curvature of each petal tip.

magnitude. The Fresnel number range of 4.7–120 is selected for the geometry of the on-axis design of the eLISA telescope.

D. Petal-shaped masks with 2, 5, and 10-mm diameters

The 2-mm diameter masks are designed with 6, 8, 12, and 16 petals. The shape of each mask is specifically designed to maintain sharpness of the petal tips between 2 and 200 μm. The fabricated masks on substrate are photographed under microscope and the outer ROC of petal tips is recorded. The 6-petal mask shows very close agreement with the designed 2-μm tip. The masks in this set are designed to suppress the intensity at Fresnel number of 4.7. The outer ROC of the petal tips on the fabricated 8, 12, and 16-petal masks shows less agreement with the prescribed tip ROC.

The 5-mm diameter masks in this set have the same number of petals as the smaller size masks. The petal tips are designed between 2-μm and 2-mm in radius. The targeted Fresnel number is 29.3. An examination of the masks shows the larger petal tips in least agreement between the measured outer ROC and prescribed petal tip radius. In particular, the fabrication of the mask with the largest ROC is not in good agreement with the design.

The 10-mm diameter masks have 6, 12, and 16 petals. The tips sharpness range from 2 μm to 2 mm. The targeted Fresnel number in this set is 117.2. A close inspection of this set shows the most agreeable masks to the designed criteria.

As the number of petals increase and ROC of the tip increases there is less agreement between the prescribed tips and measured tips. Out of fifteen fabricated cases, six of the masks show the most agreeable ROC between the designed and measured tips. These masks are shown in shaded rows in Table I.

Figure 3 shows microscopic images of chromium masks on 4 × 4-in. glass substrates. The masks are fabricated using photolithography on 500-μm thick wafers. This set of masks represents some of the best petal tips where the designed and measured tips radius-of-curvature are in close agreement.

E. Wire Electro Discharge Machining (EDM)

The wire EDM is an electro thermal production process in which thin single-strand metal wire in conjunction with deionized water enables cutting through metallic materials by the use of heat from electrical sparks. The EDM machining works by creating an electrical discharge between the wire or electrode and the workpiece. As the spark jumps across the gap, the material is removed from both the workpiece and the electrode. To stop sparking process from shorting out, a non-conductive fluid or dielectric (deionized water) is also

TABLE I. Designed dimensions and petal tip sizes of masks fabricated using photolithography. The boldface entries are the most agreeable masks that could be fabricated using photolithography.

Mask number	Petal outer ROC (μm)	Measured petal outer ROC (μm)	Mask diameter (mm)	Measured mask diameter (mm)	Fresnel number	Number of petals
2.1	2	6	2	2.0	4.7	8
2.2	200	127	2	2.0	4.7	16
2.3	**20**	**18.4**	**2**	**2.0**	**4.7**	**12**
2.4	2	4.5	2	2.0	4.7	12
2.5	**2**	**2**	**2**	**2.0**	**4.7**	**6**
5.1	2	3.7	5	4.9	29.3	6
5.2	2	5.7	5	5.0	29.3	12
5.3	**20**	**27.5**	**5**	**5.0**	**29.3**	**12**
5.4	200	168	5	5.0	29.3	16
5.5	2000	767	5	5.0	29.3	8
10.1	**2**	**3**	**10**	**9.9**	**117.2**	**6**
10.2	2	6	10	9.9	117.2	12
10.3	**20**	**20**	**10**	**10.0**	**117.2**	**12**
10.4	**200**	**192**	**10**	**10.0**	**117.2**	**16**
10.5	2000	806	10	10.0	117.2	16

TABLE II. Mask shapes manufactured using wire EDM. The a.12 and a.22 masks share the same outer radius of curvature but deeper inner radius of curvature.

Mask number	Petal outer ROC (μm)	Measured petal outer ROC (μm)	Mask diameter (mm)	Measured mask diameter (mm)	Fresnel number	Number of petals
a.11	20	67	5	5.0	7.3	8
a.12	20	50	5	5.0	7.3	8–Ext
a.21	20	34	5	5.0	7.3	16
a.22	20	30	5	5.0	7.3	16–Ext

applied. The wire does not touch the workpiece so there is no physical pressure on the surface and it prevents the damage and distortion. Because of the inherent properties of the process, the wire EDM can easily machine complex parts and precision components out of hard conductive materials. The final masks using wire-EDM required ultrasonic cleaning to remove the residues from the boundaries of the mask. Handling of these masks is very delicate and petal tips with 30 μm can be susceptible to breakage. Table II shows the dimensions of the masks manufactured using wire EDM.

The masks designed in this technique were targeted toward the Fresnel number of 7.3. The two sets of masks with 8 and 16 petals manufactured in this process differed by the sharpness of the inner radius of curvature. The inner radius of curvature refers to the spacing where each petal is attached to the main body of the mask. The major goal of this exercise was to assess the performance of the wires in the tight space between the petals. Figure 4 shows a set of petal-shaped masks fabricated at Goddard's Advanced Manufacturing Branch using wire EDM. The aluminum masks are about 1 mm thick and 5 mm in diameter. Four sets of 8 and 16-petal masks were fabricated. The manufactured masks had 30–67 μm radius of curvature for a designed 20-μm tip.

III. EXPERIMENT

The performance of the masks was evaluated in an optical testbed setup in the laboratory as shown in Figure 5. The flywheel of masks was mounted on a pedestal post along the optical axis between laser source (1064 nm) and Coherent LaserCam-HR progressive scan CMOS detector with 6.7 μm pixel size. A series of dark images are taken while the overhead lights and laser source turned-off to capture the ambient light in the lab. These images were subsequently subtracted from the images of the laser source and the mask images as "background." This process removes the presence of any ambient light present from the detector during the experiment. The laser beam originates from a source and gets collimated before it covers the whole area of the mask and the detector. A beam expander, visually checked using a shear plate, was used to produce a one-inch diameter beam. The position of the mask could be varied from 27 cm to 82 cm away from the detector. This is equivalent to Fresnel number between 4.7 and 120. The relationship between Fresnel number and the distance between detector and mask is derived from $z = R^2/f\lambda$, where R is the radius of mask, f is the Fresnel number, and λ is the wavelength of the incident beam. A subset of 2-mm diameter masks (mask 2.3 from Table I) was evaluated in this setup by rotating the flywheel disk and aligning a desired target mask into the optical path between the laser and the detector. This setup allows quick insertion and change of the mask into the beam path.

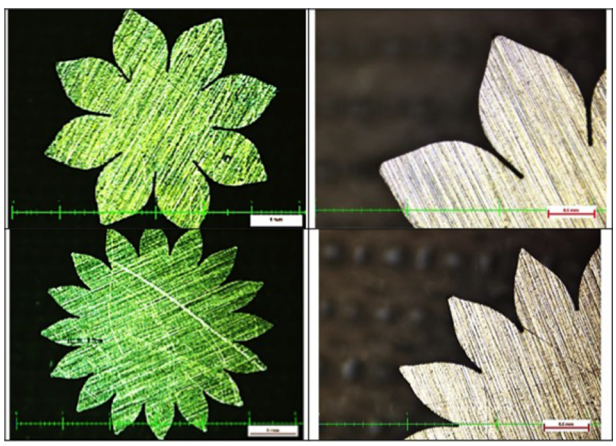

FIG. 4. The aluminum masks of about 5-mm in diameter were fabricated using wire EDM at Goddard's Advanced Manufacturing Branch. The thickness of the mask is about 1 mm. The right column is zoomed microscopic image showing the curvature of each petal tip.

IV. RESULTS AND DISCUSSION

In this work, we used four readily available techniques to fabricate petal-shaped masks. The shapes produced by the inkjet printer have rough edges and large spatial gaps on the surface of the mask making them impractical for optical testing. The 3D additive printing shapes have imperfect rough boundaries that are far from the prescribed models making them of a lower quality. The photolithography fabrication

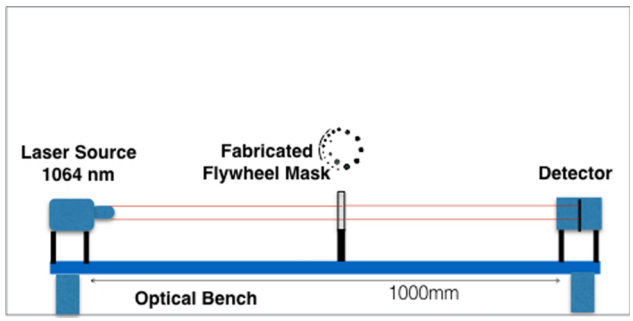

FIG. 5. Optical testbed setup used for testing the intensity suppression of flywheel mask.

produces the sharpest masks. The manufacturing tolerance on the petal tips is about 1/10 of μm. Assessing the fabricated masks solely on the measured outer radius of curvature (ROC) and designed ROC, lithography fabricated 2 and 10 mm diameter masks represent the optically preferred masks (Table I). The 5-mm diameter masks are the farthest from the designed shapes while the 10-mm diameter masks achieved the best match. The petal masks manufactured using wire EDM are not as accurate as the photolithography masks. Our wire EDM fabrication experience is limited to 5-mm diameter masks with sharp tips of 20 μm. Based on this study, we believe the key parameters to look for when choosing a fabrication technique, that is, those characteristics that appear to make the best masks are (a) closely spaced high-resolution printing nozzles and (b) accurate tracking and scaling capabilities.

The optical performance of the masks is measured and compared against the mathematical model. Figure 6 shows the logarithm of the relative intensity suppression, as the ratio of the intensity at the shadow to the intensity of the incident beam, of a 2-mm diameter 12-petal mask (mask number pmask 2.3 from Table I). The mask position along the optical axis varied from 27 cm to 82 cm. The measured intensity (red) qualitatively follows the prediction (blue) as expected. The maximum suppression of about 4 orders of magnitude occurs at z = 27 cm. Based on this experiment we do not think there was any problem with scattered light. If there was substantial scattered light it's effect would be largest at the spot closest to the detector since the solid angle subtended by the detector is largest. However, we get the best results at the shorter distance.

The cross section profile of the intensity in the shadow region was also measured at each position along the optical axis. Figure 7 compares the intensity across the 12-petal mask at 27 cm away from the detector. The plot shows the intensity of incident laser beam (black), circular mask (blue), and 12-petal mask (red). The intensity in the shadow of a circular mask shows the presence of a Poisson spot, and successful suppression by the pmask 2.3 by 4 orders of magnitude across the petal mask. The measured suppression shown at the shadow region is limited to the dynamic range of our detector. We expect the suppression to be higher and we are working to improve the dynamic range.

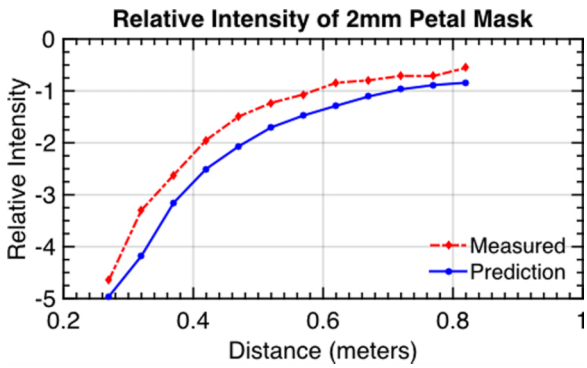

FIG. 6. Relative intensity in the shadow region of a 12-petal mask. The intensity measurement was taken at distances of 27 cm–82 cm between the mask and the detector.

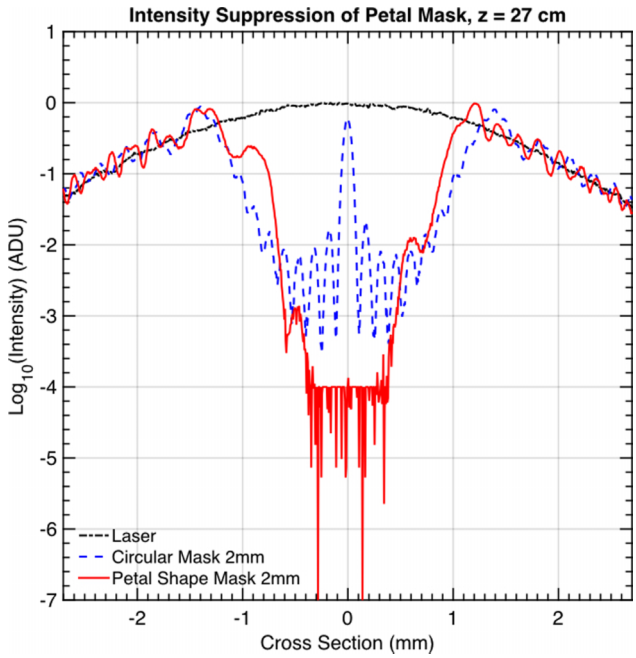

FIG. 7. Intensity suppression of petal-mask. The intensity is normalized to the center of the incident laser source of 1064-nm (black). The Poisson spot due to a circular mask (2-mm diameter) is shown (blue). The distance between the petal mask and detector is 27 cm. The intensity suppression of 12-petal mask is 4 orders of magnitude. The dynamic range of the detector is one of the limiting factors in achieving higher suppression.

V. CONCLUSION

In this study, we fabricated a series of petal-shaped masks from 2 mm to 50 mm in diameter designed to suppress the intensity along the optical axis with Fresnel numbers in the range of 4.7–120. A variety of fabrication techniques (e.g., high resolution inkjet, 3D printer, photolithography, and wire EDM) were used in this work. The masks fabricated using inkjet and 3D printing portray a number of deficiencies such as spatial gap on the opaque surface of the mask and rough boundaries that makes them unsuitable for high intensity optical application. The photolithography-fabricated aluminum masks on fused silica wafer produce accurate and sharp petal-tips even at 2-μm. In our latest fabrication batch, one-sided AR coated substrate deposited with 300-nm thick aluminum shows no signs of transmission leakage of the laser source through the mask. The wire EDM manufactured masks used in this study did not produce micron-scale optically smooth petal tips. However, this cannot be a refutation of the technique since our work is limited to 5-mm diameter masks with micron-size petal tips. Table III shows a summary of fabrication techniques and achievable ROC for outer petal tips using photolithography and EDM.

This work shows the photolithography is the best technique out of the ones we have tested for reproducing the petal shape masks. But, improvements in the wire EDM may rise to the challenge soon enough for the fabrication of the sharp petal tips.

A preliminary assessment of the optical performance of the photolithography-fabricated masks to suppress the Poisson spot is conducted in an optical testbed. The position of the mask relative to the detector is adjusted to produce Fresnel

TABLE III. Summary of fabrication techniques and achievable petal tip ROC.

Method of fabrication	Diameter of mask (mm)	Achievable petal outer ROC	Mask material and thickness	Edge smoothness (μm)	Remarks
High-resolution printers	50	0.1–5 mm	Pigmented ink on mylar ~500μm	>100	High-resolution printer masks have rough edges and large spatial gaps on the surface that make them impractical for optical testing
3D printers	15–50	0.5–5 mm	Polymer resin 0.5–2 mm	>100	3D printing masks have imperfect rough boundaries that are far from the prescribed models making them of a lower quality unsuitable for optical testing
Photo lithography	2–10	2–5 μm	Chromium 60 nm and aluminium 300 nm on fused silica	<1	Lithography achieves the best result when mask diameter is small with smooth edges and sharp tips. This is the best technique out of the ones we have investigated and it is scalable
EDM	5	20 mm	Aluminium 1 mm	>1	The EDM manufacturing was conducted only on 5 mm diameter masks. This technology is not mature enough to achieve smooth edges suitable for optical performance

numbers from 4.7 to 120. Initially a 2 mm circular mask was employed to block the incident beam and intensity in the shadow was measured to verify the presence of the Poisson spot. Subsequently, 12-petal mask with 2 mm in diameter was used to suppress the bright spot. Our results show a good agreement between prediction and experiment. The efficacy of the mask is verified against the analytical model by measuring the highest suppression (4 orders of magnitude) at the position of the mask placed 27 cm away from the detector, closely following the prediction model. Even though we are limited by the dynamic range of our detector, the theoretical suppression of the designed masks is higher than our measurement.

Follow up to this work is to improve the dynamic range of the detector and to investigate coating of the masks using carbon nanotubes (CNTs). One of the applications of petal-shape masks is to suppress the intensity along the axis of light in the geometrical shadow of the secondary mirror of an optical telescope. For this purpose, the masks need to operate in a reflective mode where the incident light is considerably attenuated. Coating of the surface of petal-shape masks with CNTs should improve the suppression of incident beam. We also plan to test the masks in reflection as well as transmission.

ACKNOWLEDGMENTS

This work is supported in part through NASA Grant 11-SAT11-0027 NNH11ZDA001N "Research Opportunities in Space and Earth Sciences" (ROSES-2011) for Strategic Astrophysics Technology (SAT).

[1]J. E. Harvey and J. L. Forgham, "The spot of Arago: New relevance for an old phenomenon," Am. J. Phys. **52**, 243–247 (1984).
[2]R. G. Lyon, S. Heap, A. Lo, W. Cash, G. D. Starkman, R. J. Vanderbei *et al.*, "Externally occulted terrestrial planet finder coronagraph: Simulations and sensitivities," Proc. SPIE **6687**, 668719 (2007).
[3]J. C. Livas, P. Arsenovic, J. A. Crow, P. C. Hill, J. M. Howard, L. T. Seals *et al.*, Opt. Eng. **52**, 091811 (2013).
[4]S. R. Sankar and J. C. Livas, Proc. SPIE **9143**, 914314-7 (2014).
[5]W. Cash, "Detection of earth-like planets around nearby stars using a petal-shaped occulter," Nature **442**, 51–53 (2006).
[6]S. Shiri and W. Wasylkiwskyj, "Poisson-spot intensity reduction with a partially transparent petal-shaped optical mask," J. Opt. **15**, 035705 (2013).
[7]W. Wasylkiwskyj and S. Shiri, "Limits on achievable intensity reduction with an optical occulter," J. Opt. Soc. Am. A **28**, 1668–1676 (2011).